

We are IntechOpen, the world's leading publisher of Open Access books Built by scientists, for scientists

6,900

Open access books available

186,000

International authors and editors

200M

Downloads

Our authors are among the

154

Countries delivered to

TOP 1%

most cited scientists

12.2%

Contributors from top 500 universities



WEB OF SCIENCE™

Selection of our books indexed in the Book Citation Index
in Web of Science™ Core Collection (BKCI)

Interested in publishing with us?
Contact book.department@intechopen.com

Numbers displayed above are based on latest data collected.
For more information visit www.intechopen.com



Failure Investigation of Gas Turbine Generator Cooling Fan Blades by Experimental and Numerical Analysis

Ali Jahangiri

Power & Water University of Technology (PWUT)

Iran

1. Introduction

In gas turbine power plants, a fan is used as a cooling system to dissipate generated heat in coils (copper conductors) and generator electric circuits at the end sides of its rotor. The general map of generator has been shown in figure 1. The entrance and exit path of air for cooling has been seen in this map. The cooler air rotates in one close cycle, in this manner, the air after passing from inside of rotor, exits from the top of generator, and with passing from one cooler, cools with water flow. The air after cooling, conducts to rotor from two sides and by the fans that are set up on the Retaining Ring, is blown in two sides of rotor.

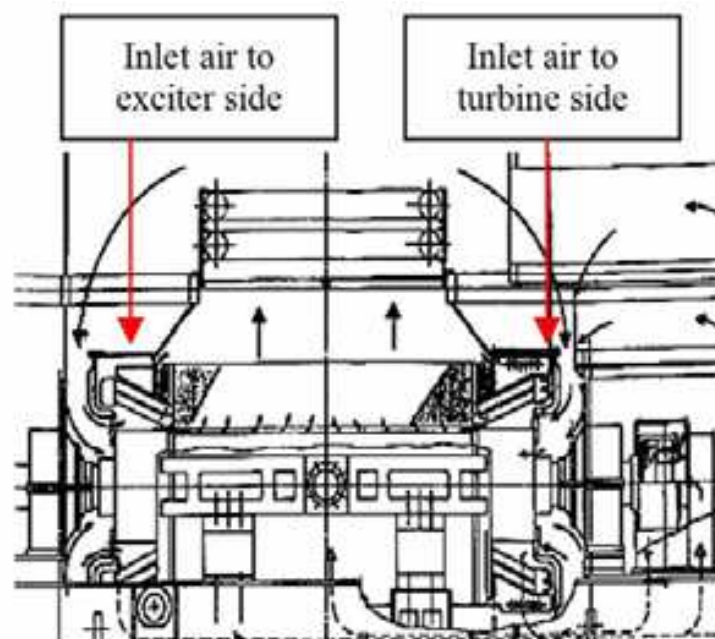


Fig. 1. Generator diagram

At each of two sides of generator sets up 11 blades as an axial fan that separates with 11 spacer pieces. Position and arrangement of blades and spacer pieces on Retaining Ring is shown in figure 2.

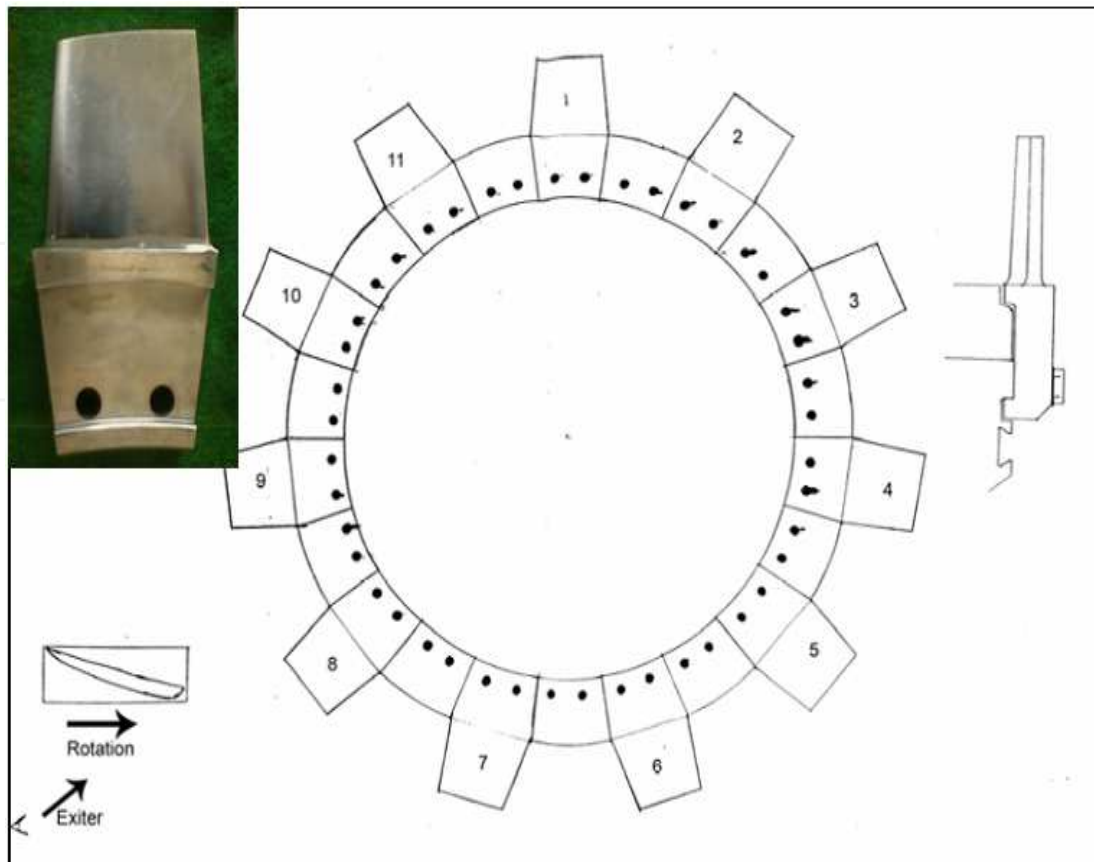


Fig. 2. Arrangement of blades around Retaining Ring

It is obvious that the fan blade has effective factors on the generator performance. In some cases, fracture of blades can cause short circuit between rotor and stator and consequently generator explosion and lots of financial loss. Cooling system equipments were supplied by GEC-ALSTHOM Belford under the following conditions; Turbine rotation=3000 rpm; output power=118 MW; The fracture of cooling fan blades has been occurred five times at the turbine side of the generator in our case study, just 10 hr after resuming operation following the last overhaul.

It must be noticed that all the failed blades had the 19° angle of attack and after failure; GEC-ALSTHOM replaced them by 14° angle of attack (without change in alloy type) in order to decrease the forces made to blades. A width of 14° blades is lower than 19° , but the height of them is same. The face of two blade types is compared in figure 3.

Figure 3 defined the deference between angle and blades dimensions.

The review of pervious blade fracture analysis notes shows that it has been a serious problem in different types of blade.

Failure investigation of blade and disk in first stage compressor in an aero engine is done and Metallurgical examination and stress analysis revealed that the design shortcoming resulted in over-compensation of centrifugal bend moment and bad contact condition (Xi et al., 2000).

A series of mechanical analysis and examination on a failed blade in gas turbine engine has been performed and nonlinear finite element to determine the stress of the blade, in order to identify the case of blade failure has been utilized (Hou et al., 2002; Beisheim & Sinclair, 2002).



Fig. 3. Deference between 2 types of blade in angle and their dimensions

The efficacy of a fracture mechanics methodology to model the crack growth behaviour of fatigue nucleated cracks obtained under test conditions similar to those found in turbine engine blade attachments has been verified and Crack propagation lives has been calculated using stress results of FEM analysis (Hutson et al., 2005) the three dimensional fatigue crack in a typical military aircraft engine fan blade attachment by Franc3D has been simulated (Barlow & Chandra, 2005; Paris et al., 1961-3). Crack propagation trajectories under mixed-mode conditions have obtained using the planner and maximum tangential stress crack extension criteria.

In the following of these papers in this note we have performed two series of analyses and their results evaluated to identify the possible causes of failure:

Mechanical and experimental Investigation as follows:

1. Review of the history of the blades repairs and/or modifications (change in blade angle of attack from 19° to 14°).[fig 3]
2. Review of the history of the unit operation.
3. Material and microstructure (quantometry).
4. Metallurgical examination of the fractures to identify the metallurgical mode of failure (SEM).

Numerical analysis on 14° and 19° blades:

1. CFD analysis in order to study the imposed stresses of the fan blades due to operation.
2. Application of the finite element method for modal and harmonic analysis to calculation of the natural frequencies, stresses and Vibration.

2. Mechanical and experimental Investigation

2.1 Visual inspection

The statistical data revealed that all of these failures have happened in the first hour of operation after the first operation or repair of gas turbine, meaning that no fracture has happened after 100 hr of operation. On opening the turbine casing, three kinds of blades (for using 19° attack angle) were found. Broken blades, cracked blades and uncracked blades.

The failure was at the turbine side of the generator and there was no crack at exciter side. The failure site was in the transition radius between the blade airfoil and the blade base. Crack initiation point was at the centrally part of the airfoil on its concave surface. Some portion of the surface appeared black and pitted due to electric spark. But by changing attack angle of blades to 14° have not seen any failure. However temperature rise in generator case was been higher and it was result of decreasing in sucked air flow rate for generator cooling (Poursaeidi & Salavatian, 2009; Moussavi Torshizi et al., 2009).

2.2 Material and microstructure

Results obtained from the quantometry technique test that performed over blades show that the blade material is aluminum 2024 (table1). Also result of metallurgical examination over blades shows that blades are not produced by die casting, but rather molding, milling, shaping and finally polishing of the blades surfaces. Crystals directed in the direction of the blade length are a proof of this production method. Heat treatment performed in this blade is of the T351 heating operations (Moussavi Torshizi et al., 2009). Mechanical behaviors of aluminium 2024 are presented in table 2.

Elements	Al	Zn	Si	Fe	Mn	Mg	Cu
quantometry test	Base	0.07	0.07	0.11	0.67	1.36	3.97
Al 2024	Base	—	—	—	0.6	1.5	4.4

Table 1. Chemical composition of blade and its comparison with aluminium 2024 alloy (Joseph, 1993).

Alloy	Ultimate tensile stress σ_{ut}	Yield tensile stress σ_{yp}	Fatigue endurance limit σ_e
Al 2024	470 MPa	325 MP	140 MPa

Table 2. Mechanical strength of aluminium 2024 (ASM, 1990).

At 3000 rpm, (50Hz frequency of powerplant generators) dynamic stresses have been measured for any 14° and 19° blades, (table 3). Comparison of these stresses with the limit stresses (presented in table 2) shows that the stresses imposed to the blade are much lower from this limit and therefore there is not possibility of blade failure in normal operation conditions.

Blade number	Max.Stress in 3000 rpm
1FE	MPa 9
2FE	7.6MPa
3FE	18MPa
4FE	10.4 MPa

Table 3. Dynamic stresses in the blade (Moussavi Torshizi et al., 2009)

2.3 Study of fracture surfaces with SEM

It's obvious that one of the most important ways to investigate the failure pieces, is being failure surfaces study. This subsection engaged to inspect the failure surfaces and defining its result. While there is two possibility, gradual failure in the effect of endurance (fatigue) and / or failure in result of external material impact (Dimple Rupture).

In order to study of failure surface and compare quality of these 2 possible failure mechanism with standard failure handbook of this alloy (AL2024) to recognise failure main cause, has employed Scanning Electron Microscope (SEM).

Because of microstructure change in failure surface, SEM could have been able to prepare best high quality picture of surface with highest accuracy (scaled to X1000).

In this section, theory of fatigue failure and dimple rupture is considered and for which one of the mechanisms, one surface with area 1cm×1cm is prepared so that for first mechanism is used of same damaged blades at powerplant generator, breaking incident and also for preparing surface by another mechanism a piece with this alloy is broken with only one knock of external object impact.

2.4 Survey of failure (scaled by SEM) surfaces

With comparison between fig 4(a) and fig 4(b) that first is surface of broken blade at powerplant incident and second is broken in type of dimple rupture (breaking potholes) has been obviously seen, there is no any resemblance between these 2 mechanism of failure and quality of surfaces is quietly differvaried.

Therefore, existing lines in fig 4(a) doubtlessly has been fatigue lines. The faigue lines show that crack is initiated at one side and propagated in significant time.

This studies show that:

1. the wing is not interrupted in one moment in the effect of contact the external object.
2. crack is started from one or more point in the middle part of cave surface of wing (unsuitable quality of surface can be result of the start of crack) and is leded to interruption of it , in the effect of oscillatory loading of blade, and made progress in the time of turning.
3. however cannot declare exactly the reason of the starting of the crack.

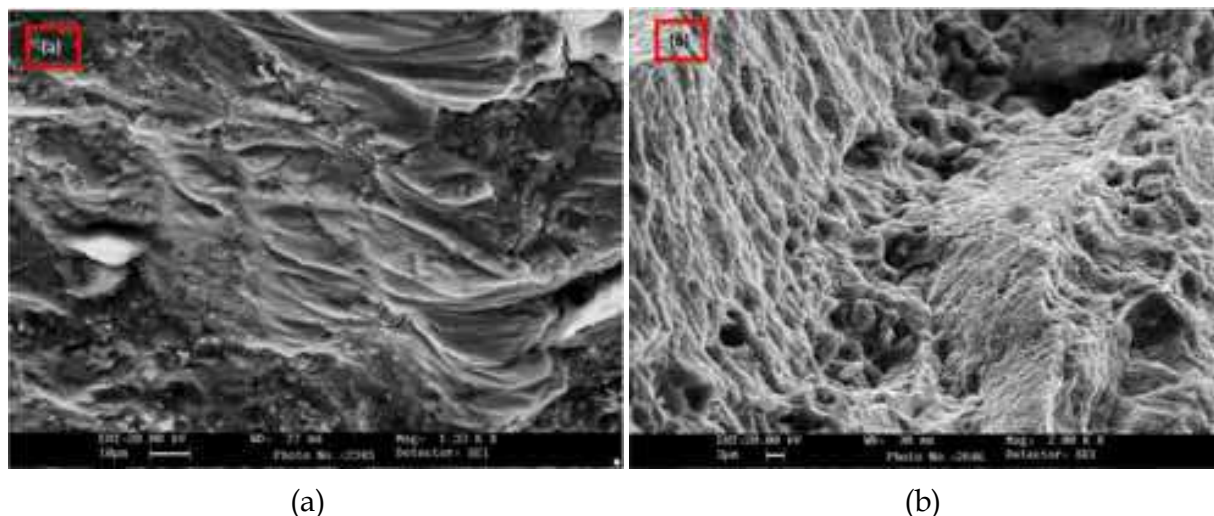


Fig. 4. (a) fatigue surface failure (scaled ×1330) (b) Dimple rupture result of instant impact (scaled ×2000)

But the contact of hard particles to wing, entrance them in the surface, creation weave centralization and the starting of crack of them is very probable.

Figure 5 has shown the final failure of surface and the ration of that to fatigue failure of surface as seen, the most of surface is created with progress crack in the effect of periodically and fatigue loads.

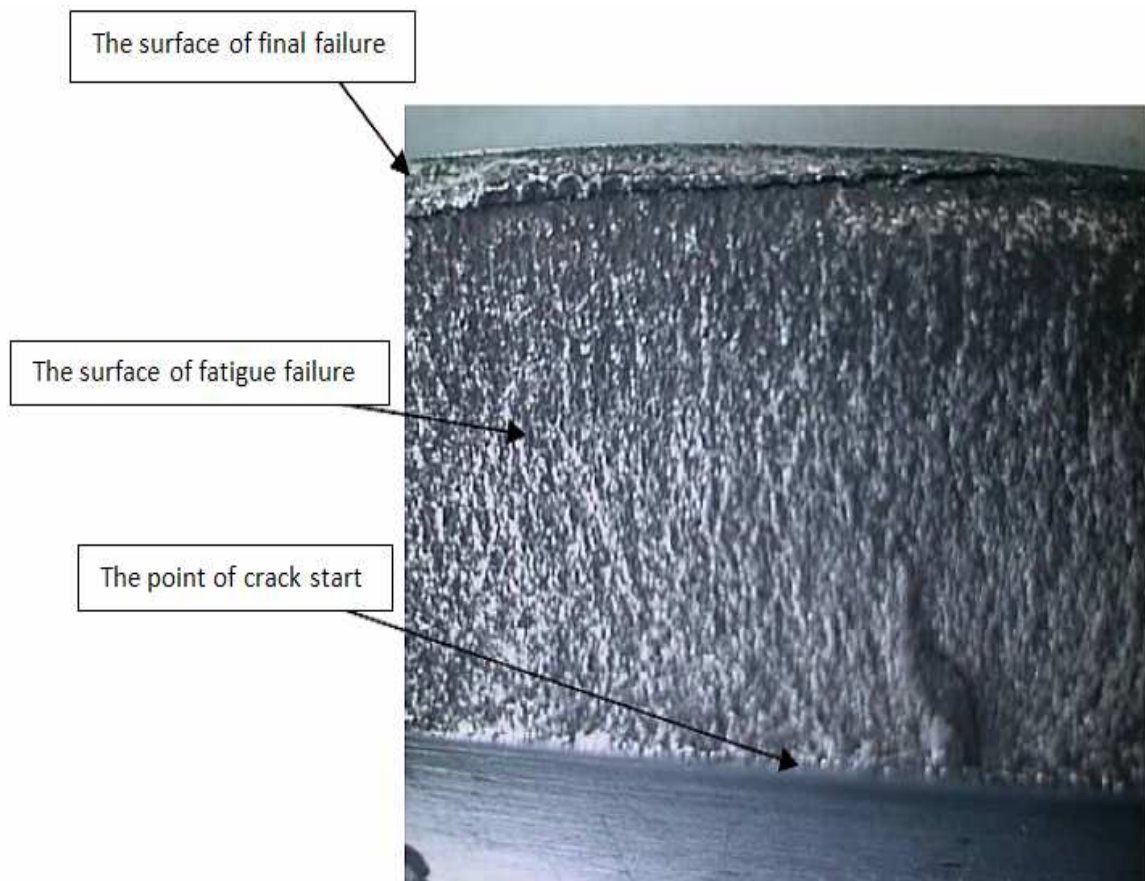


Fig. 5. Comparison between final and fatigue failure surface

3. Numerical analysis on 14° and 19° blades

In order to study the imposed stresses of the fan blades due to operation, fan should be simulated. To do this, Computational Fluid Dynamic (CFD) code and Finite Element Method (FEM) were deployed to analysis stresses and vibration. Separation phenomena and turbulent flow (vortex formation) might be cause of vibration in fan's blades.

Vibration due to oscillatory change of pressure distribution in two sides of blade may cause blade fatigue. Therefore our purpose from CFD analysis is to achieve air velocity distribution around blades and also study of air flow lines (in order to observe probable vortex and related problems) and also determination of force resulted from air pressure over blades. In this order after determination of blade profile (by using scanning digitiser camera ATOS¹ (fig 6)) modelling air passage channel is necessary, which was performed by CAD

¹ One of the new and careful methods for acquiring solid profile by digital 3d photography

software (fig 7). The 3-dimensional model thus obtained, is then imported to mesh generation software, which generates the meshing for the volume. This file as a case file could be imported to CFD code (fig 8).



Fig. 6. Scanning digitiser camera

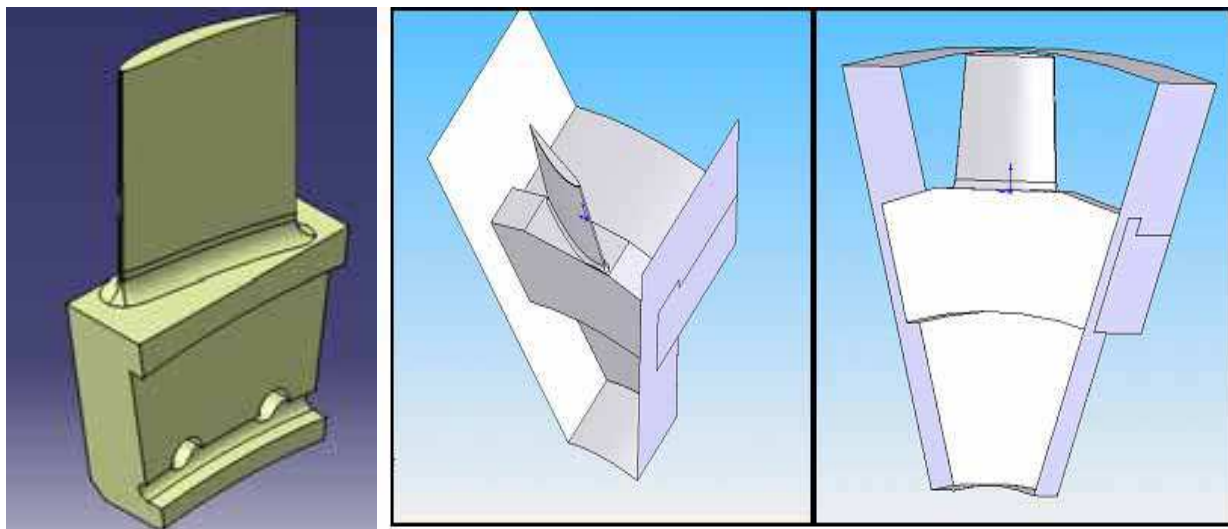


Fig. 7. 3-dimensional model of blade and related passage channel

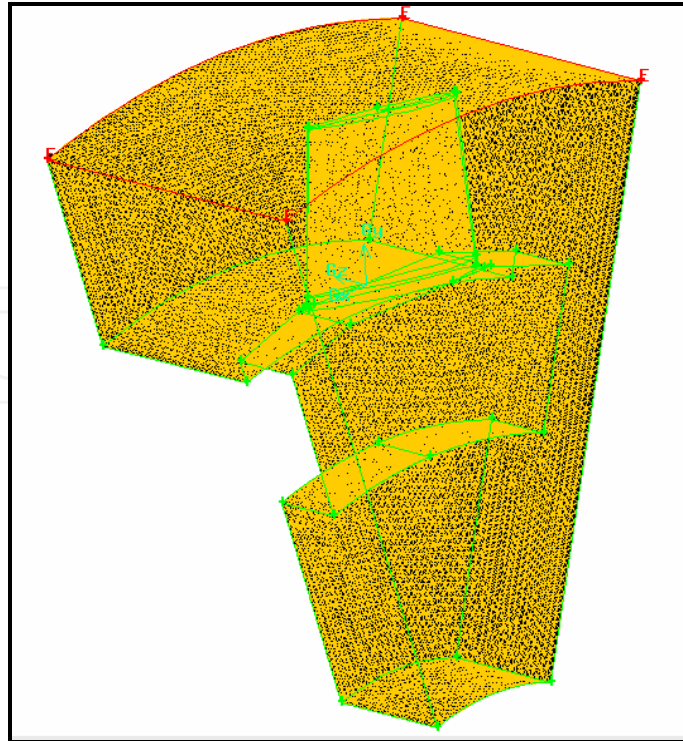


Fig. 8. Meshing domain in solution range

4. Computational Fluid Dynamics (CFD) analysis

4.1 Discretization procedure

The domain shown in Fig. 8 is divided into unstructured grids. The governing equations are solve under the boundary conditions described below by using he segregated method. Based on the finite volume method (FVM), the pressure is discretized by using the standard scheme. The momentum equations is discretized by use first order upwind scheme. The pressure-velocity coupling is treated by SIMPLE algorithm. Above discretization methods can satisfy the accuracy require under such mesh size for this problem.

"Steady state" was selected as solver and other conditions for flow and fluid are turbulent flow, compressible fluid (air) and incompressible flow (because the Mach number is less than 0.4).

4.2 Governing equations

Because of the turbulence action induced by high Reynolds swirling flow pattern, the standard k-ε two-equation turbulence model is selected and the continuity and momentum that respectively describing mass and momentum can be written as follows (White, 2003):

$$\nabla \cdot \mathbf{V} = 0 \quad (1)$$

$$(\mathbf{V} \cdot \nabla) \mathbf{V} = -\frac{1}{\rho} \nabla P + \nabla \cdot \left(\frac{\sigma}{\rho} \right) - \rho \mathbf{g} + \mathbf{S} \quad (2)$$

The turbulence equations describing turbulent kinetic energy (k) and turbulent dissipation rate (ε) are as follows:

$$(\mathbf{V} \cdot \nabla) \mathbf{k} = \nabla \cdot [(\mathbf{v} + \mathbf{v}_t / \sigma_k) \nabla \mathbf{k}] + P - \varepsilon \quad (3)$$

$$(\mathbf{V} \cdot \nabla) \varepsilon = \nabla \cdot [(\mathbf{v} + \mathbf{v}_t / \sigma_\varepsilon) \nabla \varepsilon] + c_{1\varepsilon} \frac{\varepsilon}{k} P - c_{2\varepsilon} \frac{\varepsilon^2}{k} \quad (4)$$

Here P is the generated kinetic energy of turbulence.

In these kinds of problems that a moving object is the cause of fluid flow, it is possible to take a rotational component to axial velocity of air to count blade rotation (equivalent to 314.1592 rad/s as calculated below).

$$f_r = \frac{3000 \text{ r.p.m.}}{60} = 50 \text{ Hz} \quad (5)$$

$$\omega = 2\pi \times f_r = 2\pi \times 50 = 314.1592 \text{ rad/s} \quad (6)$$

4.3 Boundary conditions

“Velocity inlet” is assumed as air entrance condition. The total volumetric flow of the cooling air is 45.6 m³/s for using 19° blade, and half of that is directed towards fan of turbine end and the other half is directed towards fan of exciter end. In inlet duct cross section, which is a circle with a radius of approximately 70 cm, velocity of air is calculated as follows (Also it should be in mind that area of air passage, is the difference between channel and generator shaft cross section):

$$Q = V \cdot A \quad (7)$$

$r_1 = 0.225 \text{ m}$ (Radius of shaft)

$r_2 = 0.696 \text{ (Radius of air channel)}$

$Q = 45.6 \text{ m}^3/\text{s}$

Then: $V = \frac{Q/2}{A} = 16.71 \text{ m/s}$

Because air pressure is uniform for all of the outlet area and along its duct, (which will be approximately equal to ambient pressure) therefore “pressure outlet” is used. For reduction of solution domain to reach to the least logical possible domain, the periodic analysis would be used.

Solution convergence accuracy have been satisfied by iterating until residuals have decreased to minimum then result could have achieved and investigated.

4.4 Analysis of flow field & pressure

As see in fig. 9 (a) & (b), in both blade type air flow pattern has been completely usual. It is observed the path lines completely tangent over the blades and the separation phenomenon has not incurred.

Air pressure distribution over blades have also seen at these two figures. Maximum absolute value of pressure that imposed to 19° angle of attack blade have reached to 56kPa on bottom of blade surface and then resultant force over the blade is approximately equal to 346N. Tension result of this force is less than amount that solely causes to break the blade.

Also in 14° blade maximum pressure at the bottom of blade is reached to 39kPa that even is less than of 19° blade.

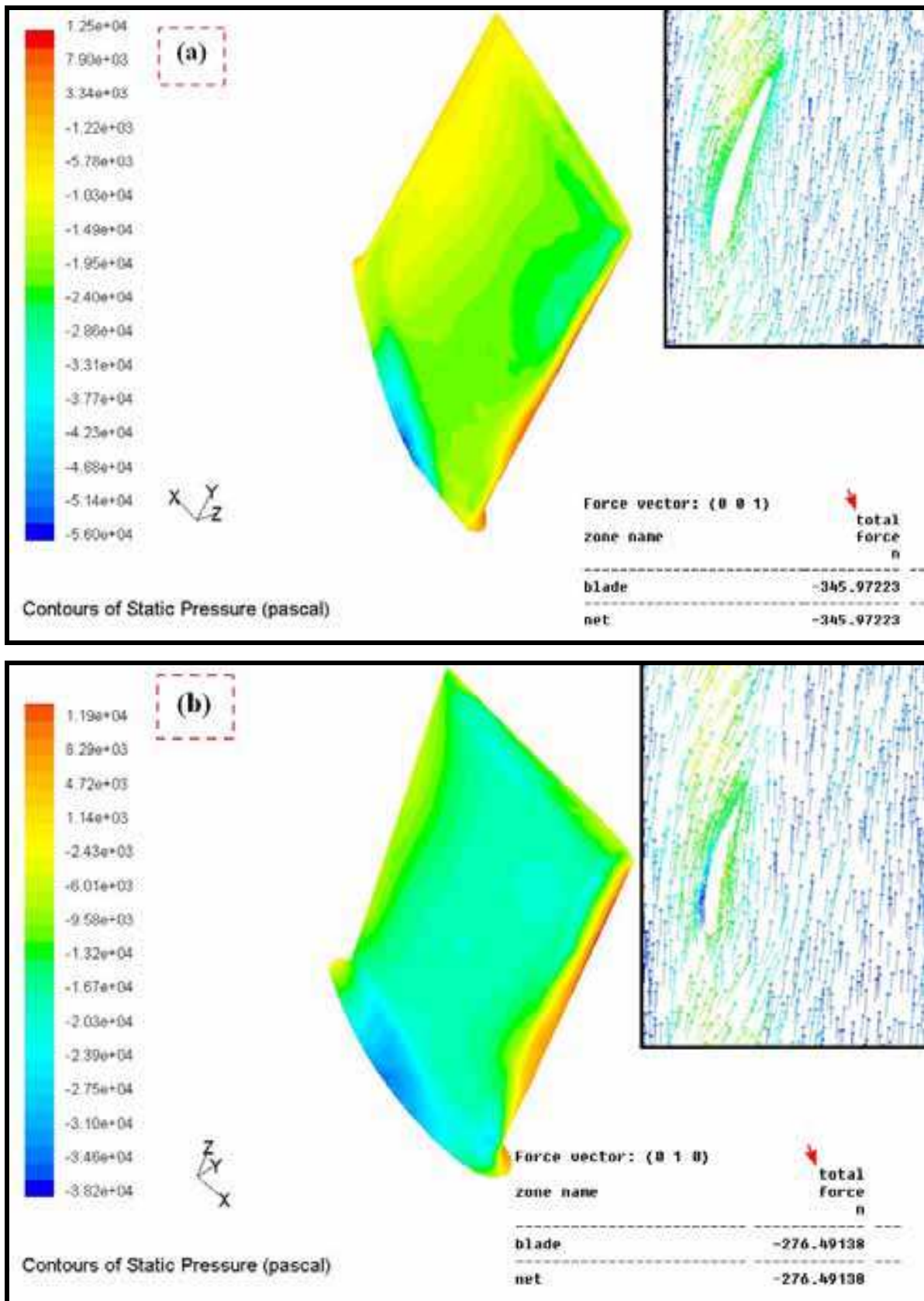


Fig. 9. (a) pressure Contour & velocity vectors passed over 19o angle of attack blade
 (b) pressure Contour & velocity vectors passed over 14o angle of attack blade

While 19° angle of attack blade has been changed with 14° blade amount of force imposed to blade would decreased about 20% and is reached from 346 to 276N then, these forces caused by air flow are not enough to cause the blade rupture.

5. Finite Element Method Analysis (FEM)

In order to determine the stresses acted on the blade and survey of the possibility of its failure caused by resonance, the finite element method, was used to blade modelling and two analysis have been performed by finite element method:

1. Modal analysis
2. Harmonic analysis

The modal analysis on natural frequency and the harmonic analysis based on different excitation frequencies were done.

5.1 Modal analysis

First, the amount of bolts tightening was modeled and its influence on blade natural frequency was studied. To evaluate these conditions, four different states were investigated for both of 19° and 14° blade:

1. All the points around the bolts are fixed.
2. All the points of the same height with bolts are fixed.
3. In addition to all the points of the same height with bolts which are fixed, the elements, which are in contact with the retaining ring, will not also move.
4. The whole blade root is fixed in all directions.

The natural frequency in the 5 modes for these four states were calculated. In table.4 these natural frequencies for fourth state in 2 blade types has been displayed.

In figure 10 and video No 1 displacement of both of blade tip at the first modal shape has shown. With respect to the fact that the first natural frequency of the 19° angle of attack blade in the fourth state (538 Hz) was very close (almost with 2% relative difference) to the frequency of the exciting force caused by shaft rotation (11 blades × 50 rad/s = 550 Hz) and therefore the incurrence of resonance in above conditions is very probable, This state has been selected for finite element harmonic numerical simulation. Whereas 19° blades is replaced with 14° blades the first natural frequency in fourth state (413.49 Hz) will not be close (with 33% relative difference) to exciting frequency and therefore resonance condition will not occurred.

Mode Shape Number	Natural Frequency (Hz) 19° blade	Natural Frequency (Hz) 14° blade
Mode No 1	537.88	413.49
Mode No 2	1339.8	1232.6
Mode No 3	2693.8	2365.9
Mode No 4	2637.1	2794.5
Mode No 5	3879.5	3837.1

Table 4. Calculated natural frequency in the 5 modes for 19° and 14° blade

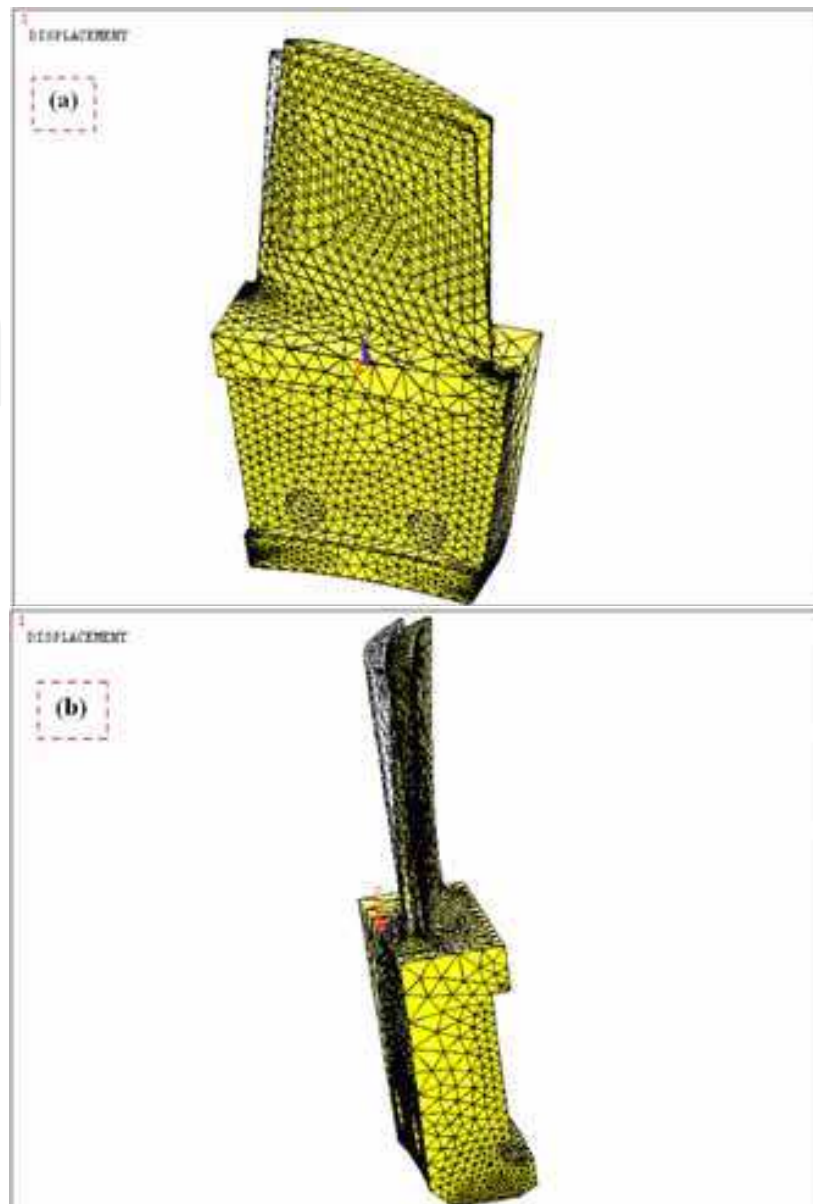


Fig. 10. (a) blade tip displacement at the first modal shape for 19° angle of attack blade
(b) blade tip displacement at the first modal shape for 14° angle of attack blade

5.2 Harmonic analysis

In harmonic analysis, the frequency of external forces (air flow and shaft rotating force) acted to blades, increases step by step, (from zero to 1000Hz) then, domain, difference shapes of vibrations and tension result of these acting external forces with, changing in blade type, account for various frequencies.

5.2.1 Harmonic analysis for 19° blade

From CFD analysis force acted by air flow on 19° blade was calculated about 346N. By acting these external forces to blade in the various frequencies (between 0 to 1000 Hz), blade tip oscillation domain (blade tip displacement), is accounted. Blade tip displacement for these conditions is shown in figure 11.

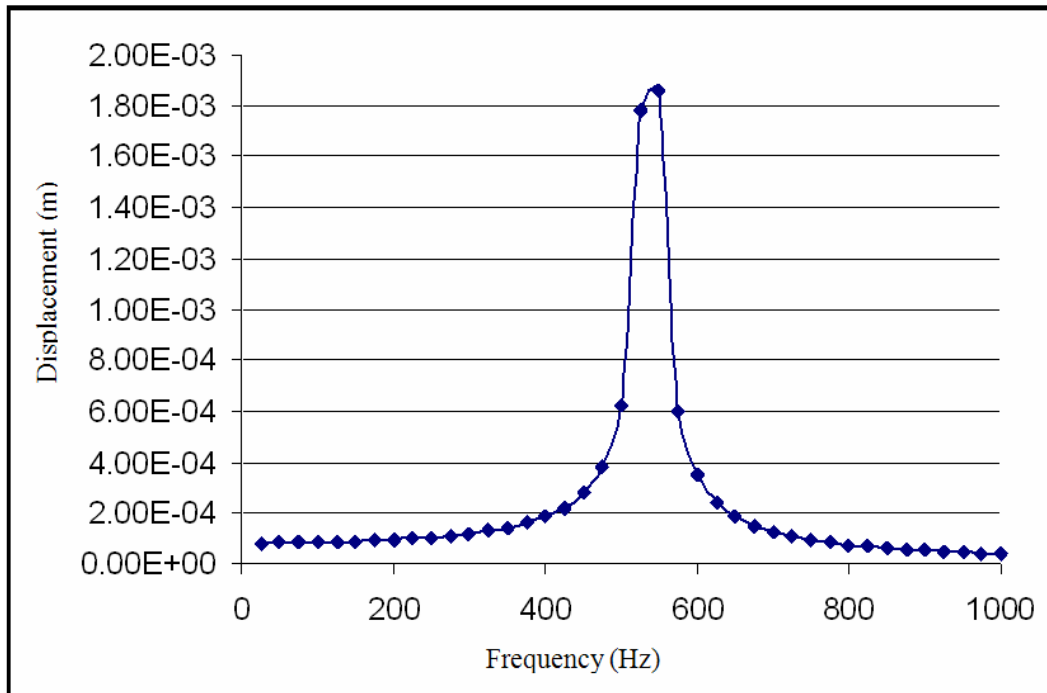


Fig. 11. 19°Blade tip displacement at various frequencies in first mode of vibration

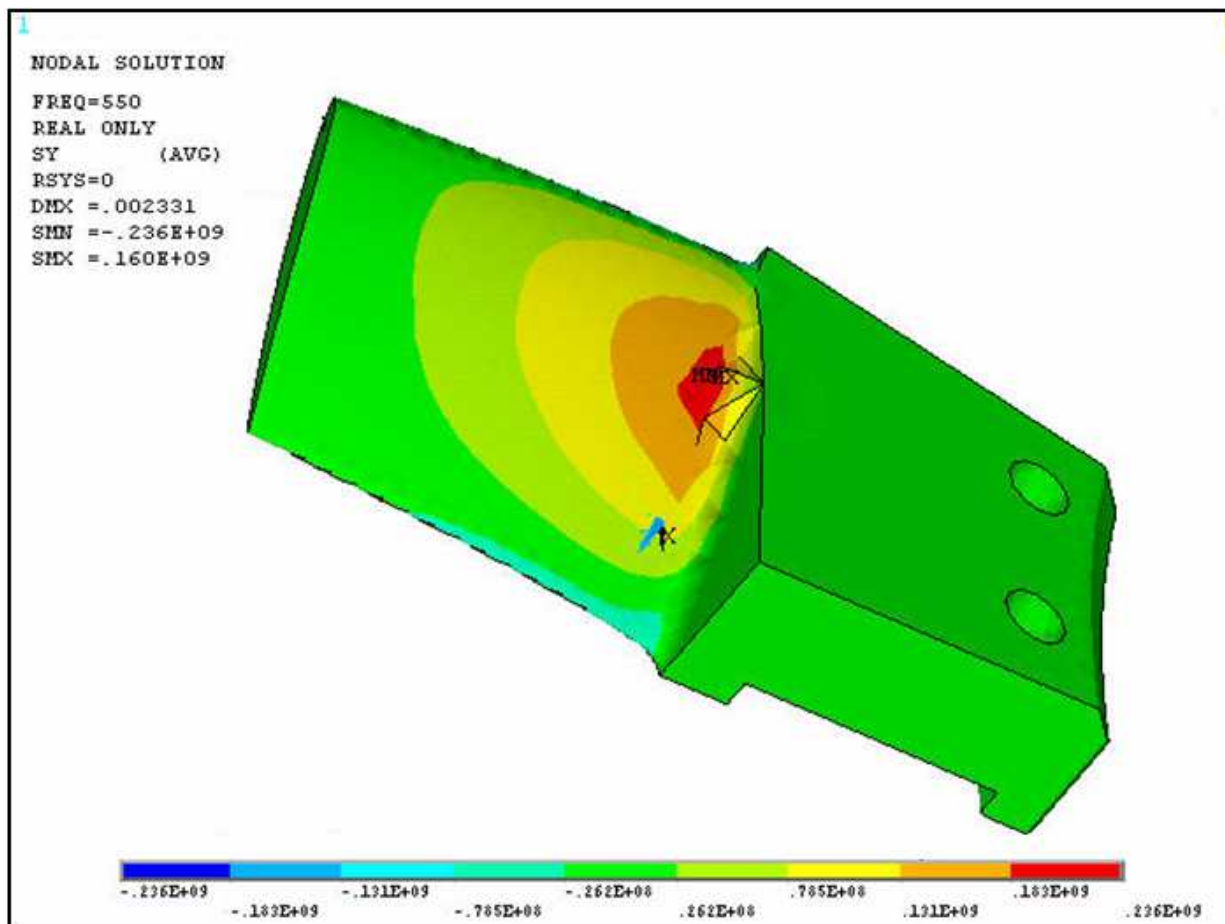


Fig. 12. Contour of computed Von Mises tension exerted on 19°Blade at 550Hz frequency

As seen, in 50Hz frequency blade tip displacement is reached to about 82 μ m this value grows with increasing frequency to the extent of 425 to 450 Hz reached to 220 to 280 μ m. In first Natural frequency vicinity, displacement is increased intensely and is reached to about 1.8mm and hereafter by frequency increasing, the blade tip displacement again decreases intensely.

With notice to figure 11 resonance condition happening will be imminent, when the blade has been excited with 550Hz frequency, that is near to first natural frequency. The blade will be vibrated intensely in this condition and as seen in fig 12, Von Mises tension at sensitive spaces of blade (blade root) is reached to 236MPa.

By referral to table 2 is been obvious that tension with amount of 236Mpa is far less than any mechanical strength of alloy except fatigue endurance limit, namely, blade material could be able to endure any forced statistical loads even at resonance state.

But thence that maximum amount of von mises tension is larger (68%) than fatigue endurance limit (236MPa > 140MPa) therefore, when blade is been encountered to fatigue condition at resonance condition, 19 $^{\circ}$ blade couldn't be able to endure fatigue condition infinitely and blade fracture will be unavoidable.

5.2.2 Harmonic analysis for 14 $^{\circ}$ blade

From CFD analysis force acted by air flow on 14 $^{\circ}$ blade was calculated about 276.5N. By acting these external forces to blade in the various frequencies (between 0 to 800 Hz), blade tip displacement, is accounted. Blade tip displacement for these conditions is shown in figure 13.

As seen, in 420Hz frequency blade tip displacement is reached to about maximum quantity (4mm) because of this reality that 420Hz frequency is nearest value to first natural frequency of 14 $^{\circ}$ blade (413.49Hz). This amount of displacement (4mm) has been even more than of 19 $^{\circ}$ blade at vicinity of its first natural frequency (1.8mm).

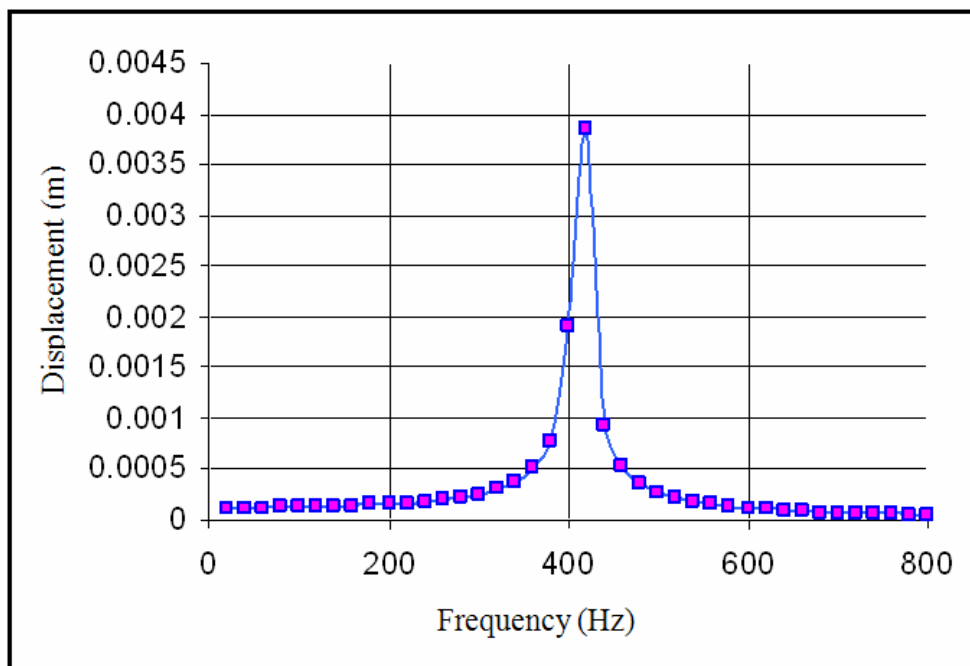


Fig. 13. 14 $^{\circ}$ Blade tip displacement at various frequencies in first mode of vibration

With notice to figure 13 in 420Hz frequency resonance condition happening will be imminent, The blade will be vibrated intensely in this condition and as seen in fig 14, Von Mises tension at sensitive spaces of blade (blade root) is reached to 388MPa. So again when 14° blade is encountered to fatigue condition at resonance condition, couldn't be able to endure fatigue condition infinitely and blade fracture will be unavoidable.

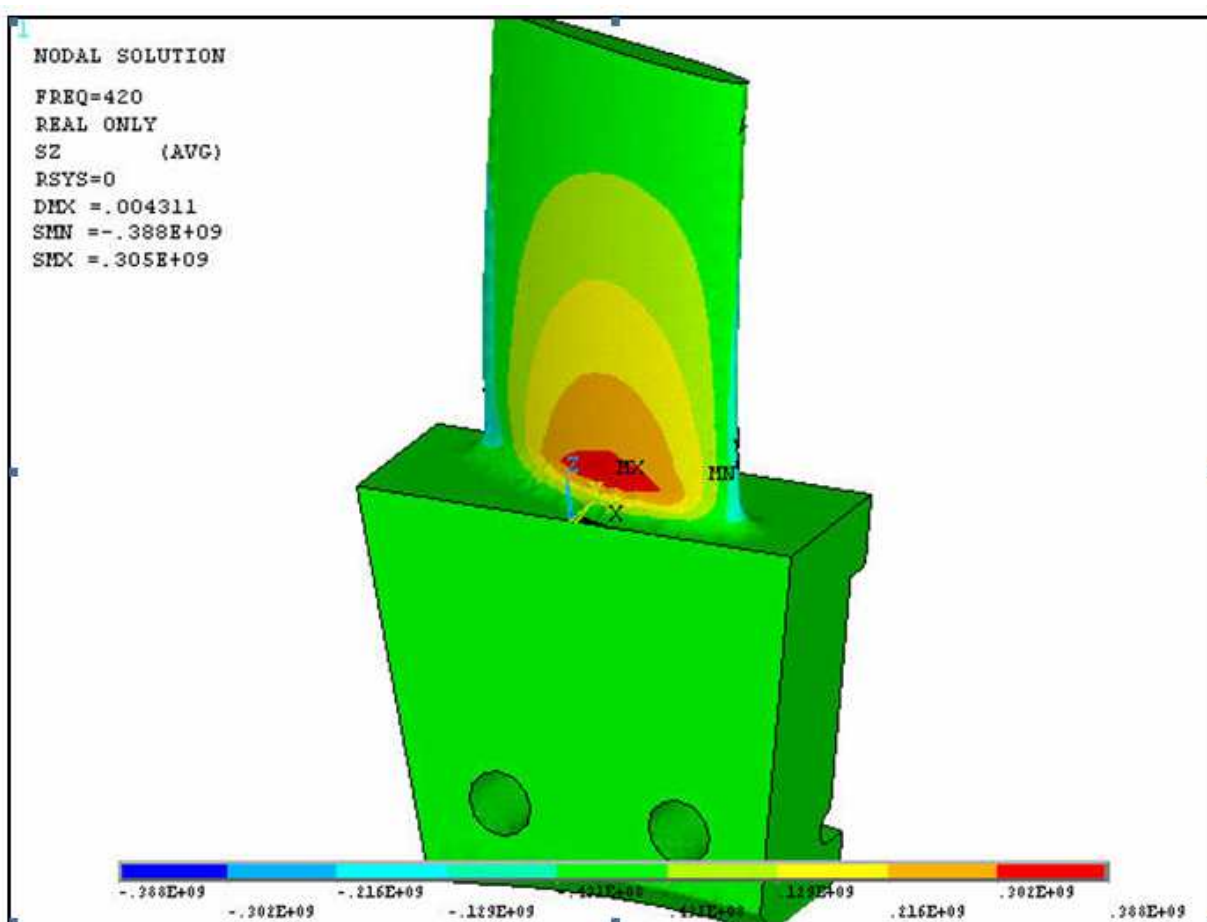


Fig. 14. Contour of computed Von Mises tension exerted on 19° Blade at 550Hz frequency

But as seen in fig 13, when the blade has been excited with 550Hz frequency, that is frequency of the exciting force caused by shaft rotation, 14° blade tip displacement will be less than 160µm. Therefore in this condition resonance state will not be happened and Von Mises tension encountered to 14° blade root will be less than 10MPa that is so small to comprised. Blade failure will never be occurred for 14° blade in this condition.

6. Conclusion

1. Experimental study of ruptured surfaces shows that the probability of a collision of a large external object and its instantaneous rupture is impossible.
2. CFD analysis shows that the forces caused by air flow are not enough to cause the blade rupture.
3. With respect to the obtained results, this analysis shows that the value of normal stress in most of conditions for 19 & 14° blades is about 10 MPa except in resonance state.

4. In the case of applying a force with a frequency of nearby 550 Hz, 19° blade will be exposed to a resonance frequency (As a result, with unsuitable blade fastening of the blade, resonance condition is probable) and because of applying stress at range of 160–236 MPa cyclically and exceeds the endurance limit of the material, it will reduce working life of the blade and lead to failure after a number of cycle.
5. In the case of applying a force with a frequency of nearby 550 Hz, 14° blade will not be exposed to a resonance condition and because of applying stress at limit of 10MPa, Blade failure will never been occurred.
6. Concerning the large number of turbines and regarding to this point that fracture happened in five case, early after operation (less than 100 h) and after the first operation or repair, and the point that if the element has not broken early after operation and has continued its usual work obtained results from CFD and vibration analysis, the most probable reason for breakage phenomenon is the way blades have been fastened (how fixed are bolts).

7. Acknowledgements

This work was supported by Semnan University (Iran, Semnan, Semnan University). and the author would like to acknowledge the energy department of Power & Water University of Technology (PWUT) for their kind cooperation. Also the author would like to express his sincere thanks to Dr Moussavi Torshizi and Dr Yadavar Nikravesh, Power & Water University of Technology, Iran, for their keen interest and encouragement for undertaking these studies.

8. References

- Anderson, T.L. (1995). *Fracture mechanics fundamental and applications*, CRC Press, 9780849316562, Colorado, USA
- Alstom Company report in conjunction with someone Gas Power Plant (1997)
- ASM.; (1990). *Asm Handbook, Properties and Selection, Nonferrous Alloys and Special-Purpose Materials, VOL 2*, ASM International, 0-87170-378-5, USA
- Barlow, K.W. & Chandra, R. (2005). Fatigue crack propagation simulation in an aircraft engine fan blade attachment. *Int JFatigue*, 27., (1661-1668)
- Beisheim, J.R. & Sinclair, G.B. (2002). On the three-dimensional finite element analysis of dovetail attachment. *Proceedings of ASME Turbo Expo*, ASME, Amsterdam
- Biner, S.B. (2001). Fatigue crack growth studies under mixed-mode loading. *Int JFatigue*, 23., (259-263)
- Erdogan, F. Sih, G.C. (1963). On the crack extension in plates under plane loading and transverse shear. *JBasic Engng – Trans ASME*, 85., (519-527)
- Failure analysis report of Iran-Montazer-Ghaem unit6. Iran Power Plant Repair Co; (2004)
- Failure analysis report of Iran-Montazer-Ghaem unit4. Iran Power Plant Repair Co; (2004)
- Failure analysis report of Iran-Neyshabour unit2B. Iran Power Plant Repair Co; (2003)
- Forman, R.G.; Shivakumar, V. & Newman, J.r.J.c. (1994). Fatigue crack growth computer program. *NASA FLAGRO*, Johnson Space Center, Houston, Texas.
- FRANC3D Menu & Dialog Reference V2.2, (2002). *The Cornell Fracture Group*, Cornell University

- Harter, J.A. (2004). *AFGROW users and guide technical manual*, Air Force Research Laboratory, AFRL-VA-WP-TR-2004, USA
- Harter, J.A. (2008). *AFGROW USERS GUIDE AND TECHNICAL MANUAL*, AFGROW Directorate, Air Force Research Laboratory, Wright-Patterson AFB, OH, AFRL-VA-WP-TR-2008, USA
- Hou, j.; Bryon, J.; Wicks and Ross A. (2002). An investigation of fatigue failures of turbine blades in a gas turbine engine by mechanical analysis. *Engineering Failure Analysis*, 9., (201-211)
- <http://www.cfg.cornell.edu/software/software.htm>
- Hutson, A. Nicholas, T. & Johnc R. (2005). Fretting fatigue crack analysis in Ti-6Al-4V, *Int J Fatigue*, 27., (1582-1589), 10-1210-12
- Jahed Motlagh, H.; Noman, M. & Eshraghi, M. (2003). *Limied section ANSYS*, Tehran university publication, Iran,.
- Joseph, R. (1993). *ASM Specialty Handbook, Aluminum and aluminum Alloys*, ASM International, 087170496X, USA (448-449)
- Mills, K.; (1993). *Metals Handbook, Volume 12, Fractography*, ASM International, 978-0-87170-018-6, USA
- Moussavi Torshizi, S.E.; Yadavar Nikraves, S.M. & Jahangiri, A. (2009). Failure analysis of gas turbine generator cooling fan blades. *Engineering Failure Analysis*, 16., (1686-1695)
- Newman, J.r.J.C. (1984). A crack opening stress equation for fatigue crack growth. *Int JFract*, 24(4)., (131-135)
- Newman, J.r.J.C, & Raju, I.S. (1984). Prediction of fatigue crack-growth patterns and lives in three-dimensional cracked bodies. *Advances in fracture research (Fracture 84), sixth international conference on fracture*, 3., (1597-1608)
- OSM. Menu and Dialog Reference, (2002). *Developed by the Cornell Fracture Group*, Cornell University, V2.2
- Poursaeidi, E. & Salavatian, M. (2007). Failure analysis of generator rotor fan blades. *Engineering Failure Analysis*, 14., (851-860)
- Poursaeidi, E. & Salavatian, M. (2009). Fatigue crack growth simulation in a generator fan blade. *Engineering Failure Analysis*, 16., (888-898)
- Rahimi ASL, R. & Soltani, M. (2003). *Calculating Fluid Dynamic (CFD) by the aid of FLUENT*, Nashre Tarrah publications
- Paris, P.C.; Gomez, M.P. & Anderson, W.E. (1961). A rational analytical theory of fatigue. *Trend Eng*, 13(1)., (9-14)
- Paris, P.C. & Erdogan, F. (1963). A critical analysis of crack propagation laws. *JBasic Eng*, 85., (528-534)
- Popov, E.P. (1968). Introduction to mechanics of solids. *Prentice-Hall*, United States of America
- Soh, A.K. & Bian, L.C. (2001). Mixed mode fatigue crack growth criteria. *Int JFatigue*, 23., (427-439)
- Steven, R.; (1993). *ASM Handbook, Volume 19, Fatigue and Fracture*, ASM International, 978-0-87170-385-9, USA
- Tada, H.; Paris, P.C. & Irwin, G.R. (1985). The stress analysis of cracks handbook. 2nd ed. St Louis, MO: *Paris Productions Inc*, 2.2.

- Vroman, G.A. (1983). Material thickness effect on critical stress intensity. *Monograph #106, TRW Space & Technology Group*
- White, F.M. (2003). Fluid mechanics. *McGraw-Hill*, United States of America
- Xi, N.S.; Zhong, P.D.; Huang, H.Q.; Yan, H. & Tao, C.H. (2000). Failure investigation of blade and disk in first stage compressor. *Eng Fail Anal*, 7., (385-392)

IntechOpen

IntechOpen



Gas Turbines

Edited by Gurrappa Injeti

ISBN 978-953-307-146-6

Hard cover, 364 pages

Publisher Sciyo

Published online 27, September, 2010

Published in print edition September, 2010

This book is intended to provide valuable information for the analysis and design of various gas turbine engines for different applications. The target audience for this book is design, maintenance, materials, aerospace and mechanical engineers. The design and maintenance engineers in the gas turbine and aircraft industry will benefit immensely from the integration and system discussions in the book. The chapters are of high relevance and interest to manufacturers, researchers and academicians as well.

How to reference

In order to correctly reference this scholarly work, feel free to copy and paste the following:

Ali Jahangiri (2010). Failure Investigation of Gas Turbine Generator Cooling Fan Blades by Experimental and Numerical Analysis, Gas Turbines, Gurrappa Injeti (Ed.), ISBN: 978-953-307-146-6, InTech, Available from: <http://www.intechopen.com/books/gas-turbines/failure-investigation-of-gas-turbine-generator-cooling-fan-blades-by-experimental-and-numerical-anal>

INTECH
open science | open minds

InTech Europe

University Campus STeP Ri
Slavka Krautzeka 83/A
51000 Rijeka, Croatia
Phone: +385 (51) 770 447
Fax: +385 (51) 686 166
www.intechopen.com

InTech China

Unit 405, Office Block, Hotel Equatorial Shanghai
No.65, Yan An Road (West), Shanghai, 200040, China
中国上海市延安西路65号上海国际贵都大饭店办公楼405单元
Phone: +86-21-62489820
Fax: +86-21-62489821

© 2010 The Author(s). Licensee IntechOpen. This chapter is distributed under the terms of the [Creative Commons Attribution-NonCommercial-ShareAlike-3.0 License](#), which permits use, distribution and reproduction for non-commercial purposes, provided the original is properly cited and derivative works building on this content are distributed under the same license.

IntechOpen

IntechOpen